

ORIGINAL ARTICLE

Comparative Studies of Renin-Null Zebrafish and Mice Provide New Functional Insights

Scott Hoffmann,* Linda Mullins¹, Sebastien Rider, Cara Brown, Charlotte B. Buckley, Adrienne Assmus², Ziwen Li³, Mariana Sierra Beltran, Neil Henderson, Jorge del Pozo, Alexandre De Goes Martini, Maria Luisa S. Sequeira-Lopez⁴, R. Ariel Gomez, John Mullins

BACKGROUND: The renin-angiotensin system is highly conserved across vertebrates, including zebrafish, which possess orthologous genes coding for renin-angiotensin system proteins, and specialized mural cells of the kidney arterioles, capable of synthesising and secreting renin.

METHODS: We generated zebrafish with CRISPR-Cas9-targeted knockout of renin (*ren*^{-/-}) to investigate renin function in a low blood pressure environment. We used single-cell (10×) RNA sequencing analysis to compare the transcriptome profiles of renin lineage cells from mesonephric kidneys of *ren*^{-/-} with *ren*^{+/+} zebrafish and with the metanephric kidneys of *Ren1*^{c/-} and *Ren1*^{ct/+} mice.

RESULTS: The *ren*^{-/-} larvae exhibited delays in larval growth, glomerular fusion and appearance of a swim bladder, but were viable and withstood low salinity during early larval stages. Optogenetic ablation of renin-expressing cells, located at the anterior mesenteric artery of 3-day-old larvae, caused a loss of tone, due to diminished contractility. The *ren*^{-/-} mesonephric kidney exhibited vacuolated cells in the proximal tubule, which were also observed in *Ren1*^{c/-} mouse kidney. Fluorescent reporters for renin and smooth muscle actin (*Tg(ren:LifeAct-RFP; acta2:EGFP)*), revealed a dramatic recruitment of renin lineage cells along the renal vasculature of adult *ren*^{-/-} fish, suggesting a continued requirement for renin, in the absence of detectable angiotensin metabolites, as seen in the *Ren1YFP Ren1*^{c/-} mouse. Both phenotypes were rescued by alleles lacking the potential for glycosylation at exon 2, suggesting that glycosylation is not essential for normal physiological function.

CONCLUSIONS: Phenotypic similarities and transcriptional variations between mouse and zebrafish renin knockouts suggests evolution of renin cell function with terrestrial survival. (*Hypertension*. 2022;79:e56–e66. DOI: 10.1161/HYPERTENSIONAHA.121.18600.) • **Supplemental Material**

Key Words: actins ■ glycosylation ■ pericytes ■ renin ■ zebrafish

The renin-angiotensin system (RAS) is responsible for blood pressure, sodium homeostasis, and water regulation. The rate limiting enzyme renin is predominantly expressed and synthesized in specialized renal, perivascular, mural cells,^{1–3} or renal lineage cells (RLCs), which are involved in renal development⁴ and have been implicated in angiogenesis of the renal vasculature.^{5–7} Mice lacking renin require neonatal subcutaneous saline

injections to survive, show recruitment of RLCs, have no detectable angiotensinogen metabolites (Ang I or Ang II), and show severe defects in renal development.^{8–10}

Studies on the RAS have predominantly focused on mammalian systems. However, the optically clear zebrafish larva contains multiple genes orthologous to the human RAS genes—angiotensin-converting enzyme (*ace*, *ace2*), angiotensinogen (*agt*), angiotensin receptors (*agtr1a*,

Correspondence to: Linda Mullins, Cardiovascular Science Centre, Queen's Medical Research Institute, University of Edinburgh, Email linda.mullins@ed.ac.uk

*S. Hoffmann and L. Mullins are joint first authors.

Supplemental Material is available at <https://www.ahajournals.org/doi/suppl/10.1161/HYPERTENSIONAHA.121.18600>.

For Sources of Funding and Disclosures, see page e65.

© 2022 The Authors. *Hypertension* is published on behalf of the American Heart Association, Inc., by Wolters Kluwer Health, Inc. This is an open access article under the terms of the [Creative Commons Attribution Non-Commercial License](#), which permits use, distribution, and reproduction in any medium, provided that the original work is properly cited and is not used for commercial purposes.

Hypertension is available at www.ahajournals.org/journal/hyp

NOVELTY AND RELEVANCE

What Is New? <p>Renin knockout delays development of the swim bladder in zebrafish larvae.</p> <p>Mice and zebrafish show vacuolation of the proximal tubule in the absence of functional renin.</p> <p>Both mouse metanephric and zebrafish mesonephric kidneys recruit renin lineage cells in the absence of functional renin.</p>	What Is Relevant? <p>Zebrafish renin lineage cells share multiple functions and comparison reveals novel mechanistic insights relating to variation in homeostatic challenges.</p> Clinical/Pathophysiological Implications? <p>The zebrafish provides important information about the evolution of renin lineage cell function. Our results suggest a continued, but noncritical requirement for renin in adult mouse and zebrafish</p>
---	---

Nonstandard Abbreviations and Acronyms	
AMA	anterior mesenteric artery
CW	conditioned water
EGFP	enhanced green fluorescent protein
JG	juxtaglomerular
RAS	renin-angiotensin system
RFP	red fluorescent protein
RLC	renal lineage cell

agtr1b, *agtr2*), renin receptor (*atp6ap2*), mineralocorticoid receptor (*nr3c2*), and renin (*ren*)—lacking only an orthologue to the Mas receptor.¹¹ Renin has been linked to teleost survival in water of fluctuating osmolarity.¹² Placing zebrafish larvae in dilute (1/20) conditioned water (CW; 60 mg/L sea salts), increases renin expression and circulating Ang II levels,^{13–15} analogous to low-salt diet administration in mammals. Despite a functional RAS, zebrafish larvae are unable to survive reduced salinity in the presence of the Ace inhibitor, Captopril.¹⁶ As in mammals, RLCs in the adult zebrafish mesonephros are present along afferent arterioles in a preglomerular position, express smooth muscle and pericyte markers, *acta2* and *pdgfrb*, respectively and are recruited under low salinity or Captopril challenge.^{17–19}

Electron microscopy of perivascular RLCs or labeling of acidic organelles with fluorescent dyes have revealed that the zebrafish RLCs contain dense core, acidic granules, suggestive of renin synthesis, storage, and processing.¹⁷ In mammals, it is thought that glycosylation sites are involved in the processing of renin and sequences encoding these highly conserved glycosylation sites are found in exons 2 and 4 of the zebrafish renin gene. However, the functional role of glycosylation in zebrafish renin remains to be elucidated.

The zebrafish *ren* transcript is first expressed in larvae at 24 hours post fertilization and has been implicated in the development of the pronephros, which is an active filtration organ from 3 dpf (days post fertilization).^{16,20} At

the larval stage, renin expression is largely limited to the anterior mesenteric artery (AMA), which supplies the swim bladder. This buoyancy aid typically becomes visible from 4 to 5 dpf, when the zebrafish larvae reach 3.4 to 3.7 mm in length,²¹ unless they are exposed to low salinity.¹³

Zebrafish kidney development terminates with the mesonephros and despite lacking the structural complexity of a metanephric kidney, nephron structure, and tubular segmentation is highly conserved and easily accessible.²² Furthermore, the zebrafish mesonephric kidney retains the ability to regenerate and restore damaged nephrons, making it an ideal model for studying renal injury and repair.^{23,24}

In this study, we generated an allelic series of *ren* mutations using CRISPR/Cas9-targeting in zebrafish. Crossing of the *ren*^{−/−} zebrafish to a double fluorescent reporter strain (*Tg(ren:LifeAct-RFP; acta2:EGFP)*), enabled high resolution imaging of the mesonephric renal vasculature, and the generation of informative scRNAseq 10× data sets. The transcriptional profiles of RLCs from *ren*^{−/−} and *ren*^{+/+} mesonephros were compared with those of equivalent mouse metanephric RLCs.

METHODS

The authors declare that all supporting data are available within the article (and its [Supplemental Material](#)). Zebrafish scRNAseq libraries have been submitted to ArrayExpress (E-MTAB-11079). Mouse scRNAseq data have been submitted to GEO public repository (GSE180873); (NCBI tracking system No. 22225156).

Detailed methods are available in the [Supplemental Material](#). All zebrafish (*Danio rerio*)²⁵ experiments were approved by the local ethics committee and conducted in accordance with the Animals (Scientific Procedures) Act 1986 in a United Kingdom Home Office approved establishment.

Statistical Analysis

Statistical analyses were performed (GraphPad Prism version 8.4.3 for Mac; GraphPad Software, San Diego, CA), by ANOVA and post hoc Sidak multiple comparisons test. Values are

reported as means \pm SD, and $P < 0.05$ was considered statistically significant.

RESULTS

Viability of Ren^{-/-} Larvae and the Pronephric Kidney

CRISPR-Cas9 targeting of G0 embryos produced chimeric founders, with a range of indels at the target site. These were resolved by backcrossing to the wild-type strain, WIK, and subsequent genotyping of F1 fish. Indels were verified by sequencing of polymerase chain reaction products²⁶ spanning the target site.

In one fish (ren^{-/-}), removal of 8 bp near the glycosylation site in exon 2 was predicted to cause a nonsense mutation, bringing a stop codon into frame in the third exon, and thus truncating the protein product (Figure S1A). F2 fish showed a Mendelian ratio of 20:38:15 (wild type: heterozygous: homozygous) indicating that homozygous knockout fish were viable in water of normal salinity (CW) and suggesting that an active RAS is not vital during early stages of development (Figure S2F).

A second knockout line, with a 9 bp deletion spanning the glycosylation site was also generated (ren^{Δ9/Δ9}), together with a knock-in line (ren^{KI/KI}), generated using an antisense ss-oligo (Figure S1B and S1C). One out of 40 fish screened carried the knock-in allele, which replaced amino acids encoding the glycosylation site, rendering it disabled. Fish homozygous for both the 9 bp deletion (ren^{Δ9/Δ9}) and the 9 bp substitution (ren^{KI/KI}) were viable.

Though viability was unaffected by loss of renin expression, a significant delay in somatic growth (length) and appearance of the swim bladder in ren^{-/-} zebrafish, was observed using the Vertebrate Automated Screening Technology system (Figure S2A). Zebrafish length was significantly reduced at 4 dpf (ren^{-/-}, 3.58 \pm 0.03 mm [n=45]; ren^{+/+}, 3.79 \pm 0.02 mm [n=29]; $P < 0.0001$), and 5 dpf (ren^{-/-}, 3.76 \pm 0.03 mm [n=37]; ren^{+/+}, 3.89 \pm 0.03 mm [n=29]; $P = 0.004$; Figure S2B). At 5 dpf, ren^{-/-} zebrafish had a dramatically reduced swim bladder size (0.055 \pm 0.006 mm², n=80) and in 42.5% cases lacked a swim bladder completely, compared with ren^{+/+} zebrafish, (0.109 \pm 0.002 mm²; n=61) which all had a swim bladder. By 8 dpf, there was still a significant difference in swim bladder area but not length of ren^{-/-} larvae compared with controls. Despite this, no obvious behavioural difference was noted.

We investigated pronephric development in ren^{+/+} and ren^{-/-} zebrafish crossed to the transgenic reporter line *tg(wt1b:EGFP)*, where Wt1b is localized to the proximal tubule and the glomerulus.²⁷ The pronephros of ren^{+/+} and ren^{-/-} *Tg(wt1b:EGFP)* zebrafish were imaged at 3-, 4-, and 5 dpf, and the anterior glomerular distance and posterior glomerular distance were measured (Figure S2C). Anterior glomerular distance and posterior glomerular distance were significantly increased in ren^{-/-} *Tg(wt1b:EGFP)* at all

3 stages of development suggesting a delay in glomerular fusion in ren^{-/-} larvae (Figure S2D and S2E). No significant difference in viability was observed when exposing ren^{-/-} zebrafish to either 1/20 CW (3 mg/L sea salt), or Captopril in CW compared with ren^{+/+} treated zebrafish. However, no ren^{-/-} zebrafish survived in 1/20 CW combined with Captopril, compared with 12.5% survival of ren^{+/+} zebrafish (Figure S2F).

Larval RLC Ablation

In larvae, renin expression is limited to the AMA, which supplies the swim bladder.¹⁶ Despite the delay in development, no significant difference was observed in the area of AMA fluorescence in the ren^{-/-}; *Tg(ren:LifeAct-RFP;acta2:EGFP)* line compared with ren^{+/+}; *Tg(ren:LifeAct-RFP;acta2:EGFP)*^{16,28} at 5 dpf, (Figure 1A through 1C; n=5 per group), suggesting that renin expression is not essential in CW.

To determine whether or not RLCs in the AMA exhibit contractile pericyte functions, we specifically ablated the RLCs in 3 dpf *Tg(ren:KillerRed)* larvae, using a Bessel beam on the SPIM microscope as previously described.²⁹ We recorded time-lapse images and measured the maximum luminal width of the AMA blood vessel, accounting for its pulsatility with each heartbeat. We demonstrated that the width significantly increased (from 19.208 \pm 1.307 μ m to 21.678 \pm 0.615 μ m; n=5; $P = 0.01$) following ablation of the RLCs (Figure 1D and 1F and Video S1³⁰).

The Ren^{-/-} Mesonephric Kidney: Renin Assay

Ang I and Ang II metabolites were predicted by comparison of zebrafish angiotensinogen protein sequence with that of higher mammals (Figure S1E), synthesized and used as standards for the indirect kidney renin assay. Ang I and Ang II were measured in pooled mesonephric kidney samples isolated from ren^{+/+}, ren^{-/-}, ren^{Δ9/Δ9} and ren^{KI/KI} fish. Results are given in Table 1. Almost no angiotensin metabolites were detected in the ren^{-/-} kidneys, confirming that renin activity is absent in these fish. Neither disabling (ren^{KI/KI}) nor removal (ren^{Δ9/Δ9}) of the glycosylation site in exon 2 affected the levels of Ang I and Ang II in their respective mesonephric kidneys.

Histology

Periodic Acid Schiff stain³¹ was used to visualize renal structures in adult zebrafish mesonephros (Figure S3A and S3B). Kidneys of ren^{-/-} zebrafish exhibited widespread, severe vacuolation of the proximal tubular epithelial cells compared with very rare, mild vacuolation in ren^{+/+} controls (n=3 per group). Absence of Periodic Acid Schiff staining suggests that the vacuoles do not contain polysaccharides or glycoproteins. No

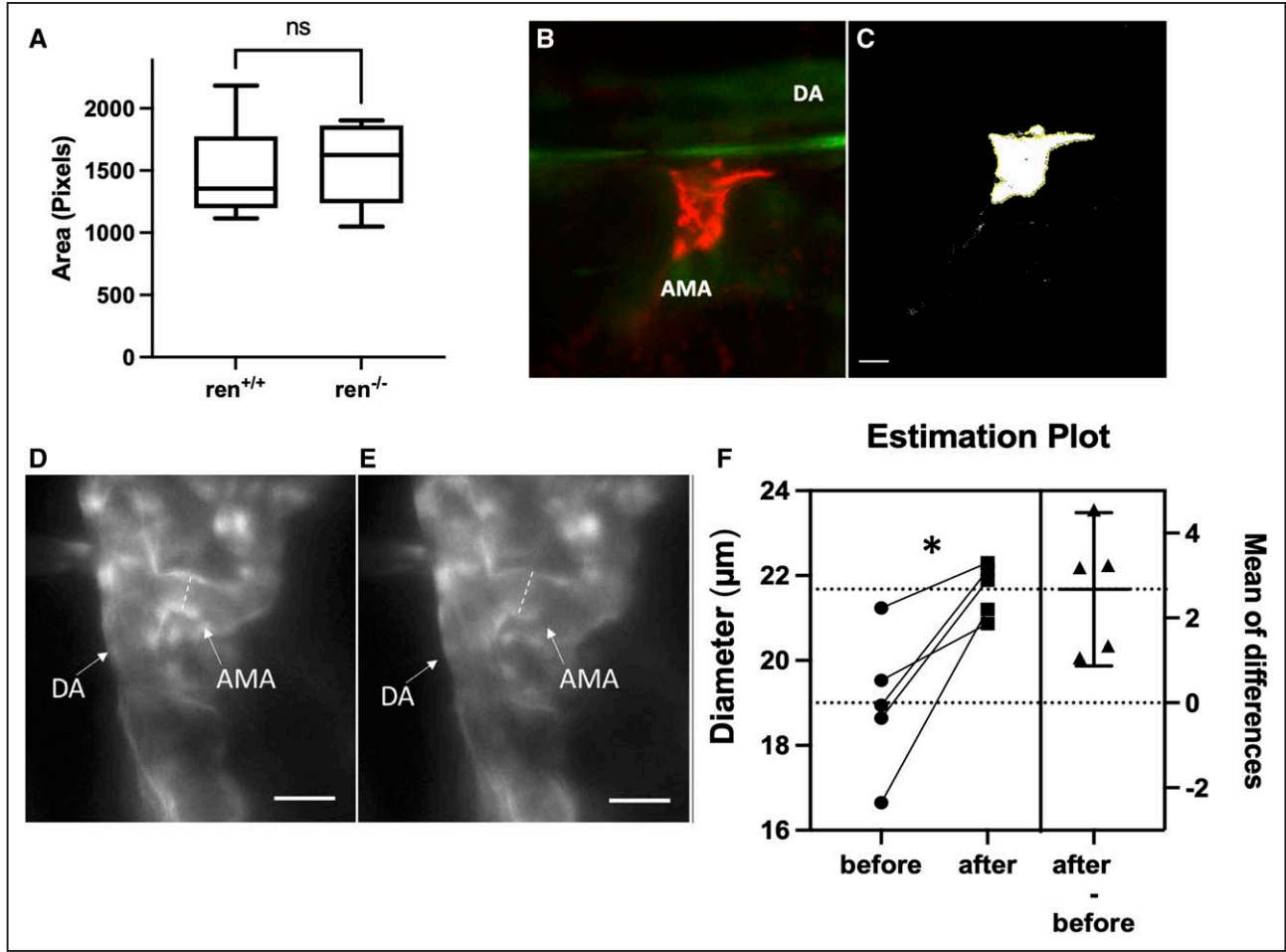


Figure 1. Anterior mesenteric artery (AMA) analysis. **A**, Quantification of the LifeActRFP fluorescent signal at the AMA in *Tg(ren:LifeAct-RFP;acta2:EGFP)* 5 dpf larvae on a *ren*^{+/+} or *ren*^{-/-} background (n=5 per group); **(B)** SPIM microscopy of pronephric AMA showing LifeActRFP (Ren-expressing cells) and EGFP (Acta2-expressing cells) fluorescence and **(C)** representative gray scale image for mean area analysis. Laser ablation of renin-expressing cells in the AMA of *Tg(ren:mem-KillerRed)* 3 dpf larvae showing *kdr:GFP* signals at **(D)** t=0 min and **(E)** t=60 min of the ablation protocol. The dorsal aorta (DA) can be seen with the AMA budding off it. Images represent single axial planes. Scale bars represent 30 μm; AMA diameter was measured at the same two locations for each fish (dotted lines); **(F)** an estimation plot and mean of differences are shown; (paired *t* test: *P*=0.0147).

differences were observed in the distal tubule, which lacks a brush border. Vacuolation of proximal tubular epithelial cells was also observed in the *Ren1*^{c-/-} mouse kidney, compared with the *Ren1*^{+/+} control (Figure S3C and S3D).

Spinning disc confocal microscopy³² of excised mesonephric kidneys isolated from *ren*^{+/+} and *ren*^{-/-} *Tg(ren:LifeAct-RFP, acta2:EGFP)* fish revealed that RLCs are located intermittently along the afferent arterioles in

ren^{+/+} fish giving a banded or striped pattern (Figure 2A). However, RFP (red fluorescent protein) labeling in *ren*^{-/-} mesonephric kidneys showed extensive continuous expression and the virtual absence of striped/banded patterning, whilst EGFP (enhanced green fluorescent protein) fluorescence, which marked smooth muscle cells, was significantly reduced (Figure 2B). This mirrors the RLC recruitment seen in mice.³³

Renin Complementation

To determine whether the *ren*^{-/-} knockout phenotype could be rescued, either by the deletion mutant *ren*^{Δ9/Δ9} or the knock-in mutant, *ren*^{KI/KI}, each was crossed with *ren*^{-/-}*Tg(ren:LifeAct-RFP, acta2:EGFP)* to generate obligate heterozygotes: *ren*^{-/Δ9}; *Tg(ren:LifeAct-RFP^{+/+}; acta2:EGFP^{+/+})* and *ren*^{-/KI}; *Tg(ren:LifeAct-RFP^{+/+}; acta2:EGFP^{+/+})*, respectively. Kidney squashes from these were assessed for complementation of the

Table 1. Angiotensin Metabolites in Mesonephric Kidneys Isolated From Zebrafish Homozygous for Mutated Renin Alleles		
Genotype	Ang 1–8, pg/g	Ang 1–10, pg/g
<i>ren</i> ^{+/+}	1159.0	6790.1
<i>ren</i> ^{-/-}	<5	<5
<i>ren</i> ^{Δ9/Δ9}	966.1	5496.0
<i>ren</i> ^{KI/KI}	1626.9	8844.9

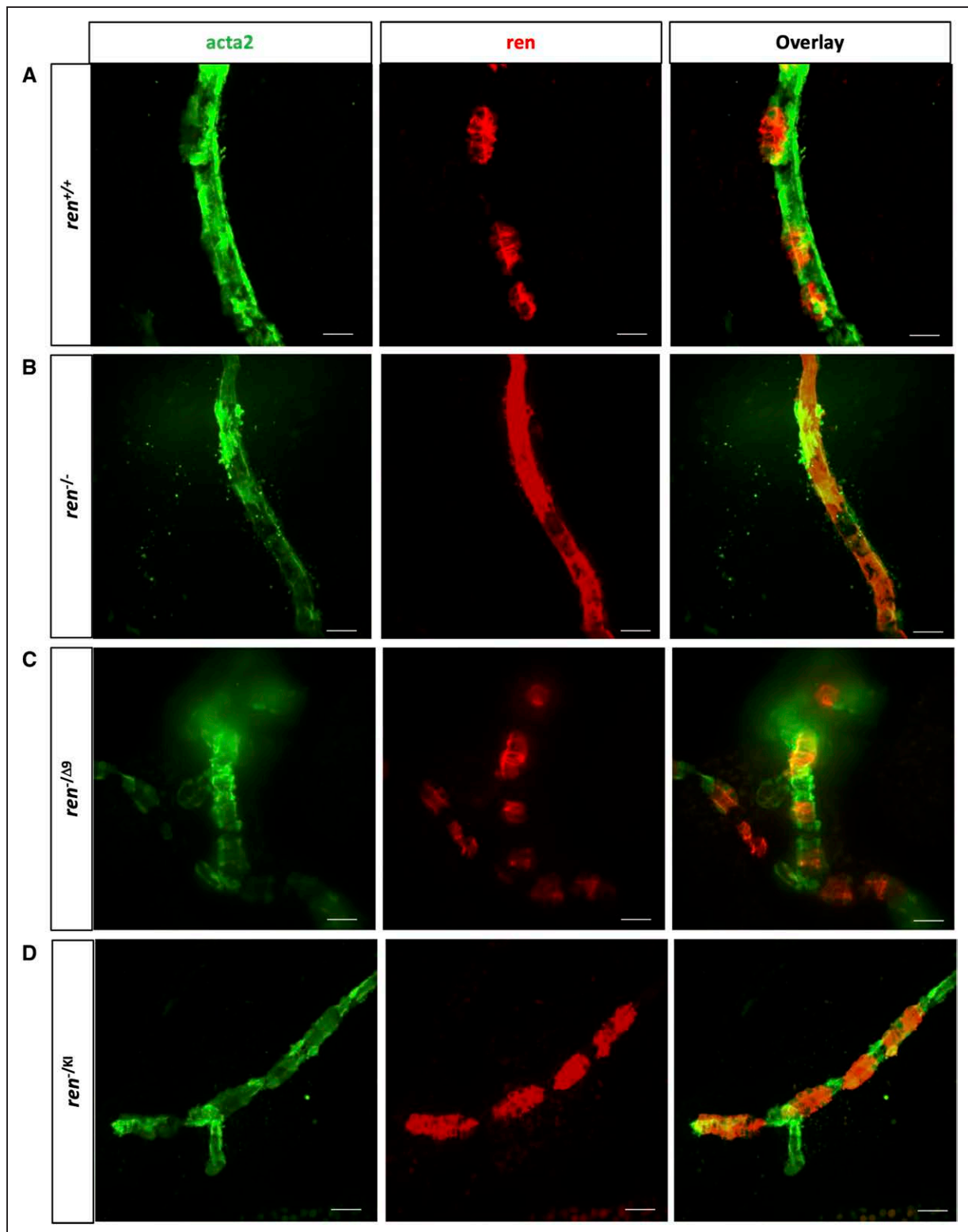


Figure 2. Spinning disc microscopy showing the expression of fluorescent reporters *ren:LifeAct-RFP* and *acta2:EGFP*. Mesonephric kidney squashes from (A) *ren*^{+/+}, (B) *ren*^{-/-} or the obligate heterozygous fish (C) *ren*^{-Δ9}, and (D) *ren*^{-/kl}. Parts show separate red, green and merged channels. Scale bar = 50μm.

banding pattern in afferent arterioles (Figure 2C and 2D). Both substitution and removal of the glycosylation site rescued the knockout phenotype.

scRNAseq Analysis

ScRNAseq 10× libraries were made from. *ren:LifeAct-RFP*⁺ and *acta2:EGFP*⁺-expressing cells,

fluorescence-activated cell sorted from *ren*^{+/+} and *ren*^{-/-} double-transgenic fish. Dimensionality reduction (t-distributed Stochastic Neighbour Embedding [tSNE])³⁴ was performed (using resolution 0.1 to set the granularity of the clustering) on the merged libraries following principal component analysis (Figure S4), and similar cells were grouped into 5 clusters (Figure S4A). Violin plots and feature plots were used to explore the transcription of key genes of interest (Figure S4B and S4C). Cluster 2 contained the majority of renin- and LifeActRFP- expressing cells while clusters 0, 1, and 2 contained *acta2*- and EGFP-expressing cells. RLCs from the control library (ZF1) represented 11.9% of the fluorescent-activated cell sorted cells, while 36.7% of cells from the RenKO library (ZF2) resided in this cluster. This probably reflects the proportion of juxtaglomerular cells from ZF1 versus the recruited RLCs from ZF2. Lists of genes differentially expressed in each cluster were generated, and several cluster 2-specific transcription factors were identified (Figure S4C) including *cnot4b*, *twist1a*, *nr2f5*, *nkx3.2*, *cited4a*, and *sox6*. Other transcripts enriched in RLCs included signaling proteins such as *angptl3* and *rgs5b*, and also *hmox1a* and *tfpia*. Pseudotime analysis³⁵ was projected onto the *seurat*-generated clusters and confirmed the relationship between smooth muscle cells and RLCs (Figure S4D).

Subsequently, cluster 2 was separated into subclusters, to identify genes that distinguish juxtaglomerular (JG) cells from recruited cells (Figure S5). Using a resolution of 0.5, 3 clusters were resolved (Figure S5A). The distribution of cells from the 2 libraries indicated that cluster C2 contains cells from the control library (ZF1) and, therefore, represents JG cells, while cells from the *ren*^{-/-} library (ZF2), representing recruited RLCs, could be divided into clusters C0 and C1. Genes differentiating the sub-clusters were interrogated further (Table 2). Transcription of *ren* was 4-fold higher in JG cells (C2) than RLCs, while transcription factors *cnot4b* and *twist1a* were upregulated in cluster 1 and *rbp4* was more highly expressed in C0 of the recruited cells (Figure S5B and S5C). The top genes listed for each cluster were assessed by gene ontology analysis (<http://geneontology.org>). C0 showed a 16-fold enrichment for transcripts related to actomyosin structural organization (including *tagln*, *acta2*, *lmod1b*, *csrp1a*), C1 showed enrichment for the vegf pathway (*vegfaa*, *pgfb*, and *gng2*) and lysosomal and lytic vacuoles, but no significant enrichment was seen in C2 (data not shown). Pseudotime mapping suggested that cluster 0 may represent a transition stage between JG cells and RLCs.

The control and knockout libraries were further analyzed using canonical correlation analysis (Figure S6; resolution 0.2 gave 8 clusters, cluster 1 containing most RLCs). This confirmed multiple genes with altered transcription in response to renin knockout, including transcription factors *cnot4b*, and *nr2f5*, and signaling factors such as *angptl3*, *rgl1*, *nedd9*, and *npr1b*. Gene ontology analysis suggested an 8.6-fold enrichment in

Table 2. Factors Involved in Transcription Control, Signaling Pathways, Actin Filament Organization and Ion Transport, Which Are Differentially Expressed Between JG cells and RLCs (Separated by Subcluster Analysis)

Cluster 0 (RLC)	Cluster 1 (RLC)	Cluster 2 (JG cell)
<i>rbp4</i>	<i>twist1a</i>	<i>cited4a</i>
<i>hmgxb4a</i>	<i>cnot4b</i>	<i>nkx3.2</i>
	<i>nr2f5</i>	<i>id1</i>
<i>acta2</i>	<i>cremb</i>	
<i>EGFP</i>	<i>fosl2</i>	<i>ren</i>
<i>myl9a</i>	<i>vegfaa</i>	<i>dio1</i>
<i>tagln</i>	<i>angptl3</i>	<i>tnmd</i>
<i>tpm1</i>	<i>rgs5b</i>	<i>tnfaip8l3</i>
<i>pfn2</i>	<i>rgl1</i>	<i>tnfsf12</i>
<i>tfpia</i>	<i>pgfb</i>	<i>regrla</i>
<i>mmp2</i>	<i>gng2</i>	<i>rasl12</i>
<i>lmod1b</i>	<i>npr1b</i>	<i>nrarpa</i>
<i>csrp1a</i>	<i>gpr137ba</i>	<i>kctd12.2</i>
<i>tpm4b</i>	<i>alkal1</i>	
	<i>sgk1</i>	
	<i>igfbp5b</i>	
	<i>cd164</i>	
	<i>socs3b</i>	
	<i>ackr4b</i>	
	<i>adora2aa</i>	
	<i>cnpy1</i>	
	<i>psap</i>	
	<i>ptn</i>	
	<i>nocta</i>	
	<i>agtrap</i>	
	<i>kcne4</i>	
	<i>clcn5b</i>	
	<i>ednraa</i>	

JG indicates juxtaglomerular cells; and RLC, renal lineage cell.

markers of lysosomes or lytic vacuoles in response to renin knockout.

Comparison of RLCs From Zebrafish and Mouse

ScRNAseq expression matrices from RLCs of the *ren*^{+/+} and *ren*^{-/-} zebrafish libraries were compared with expression matrices generated using C1 Fluidigm methodology^{36–39} on Ren1^cYFP fluorescence-activated cell sorted cells isolated from *Ren1*^{+/+} and *Ren1*^{-/-} mice respectively,^{40,41} using canonical correlation analyses.³⁴ Cluster analysis of the 2 wild-type libraries gave 2 clusters at a resolution of 0.5 (Figure 3A). Since cluster 0 included the majority of mouse and zebrafish cells, these were designated as JG like. By analogy, at a resolution of 0.6 following canonical correlation analysis of the mouse and zebrafish renin knockout libraries, cluster 0 was designated as

ORIGINAL ARTICLE

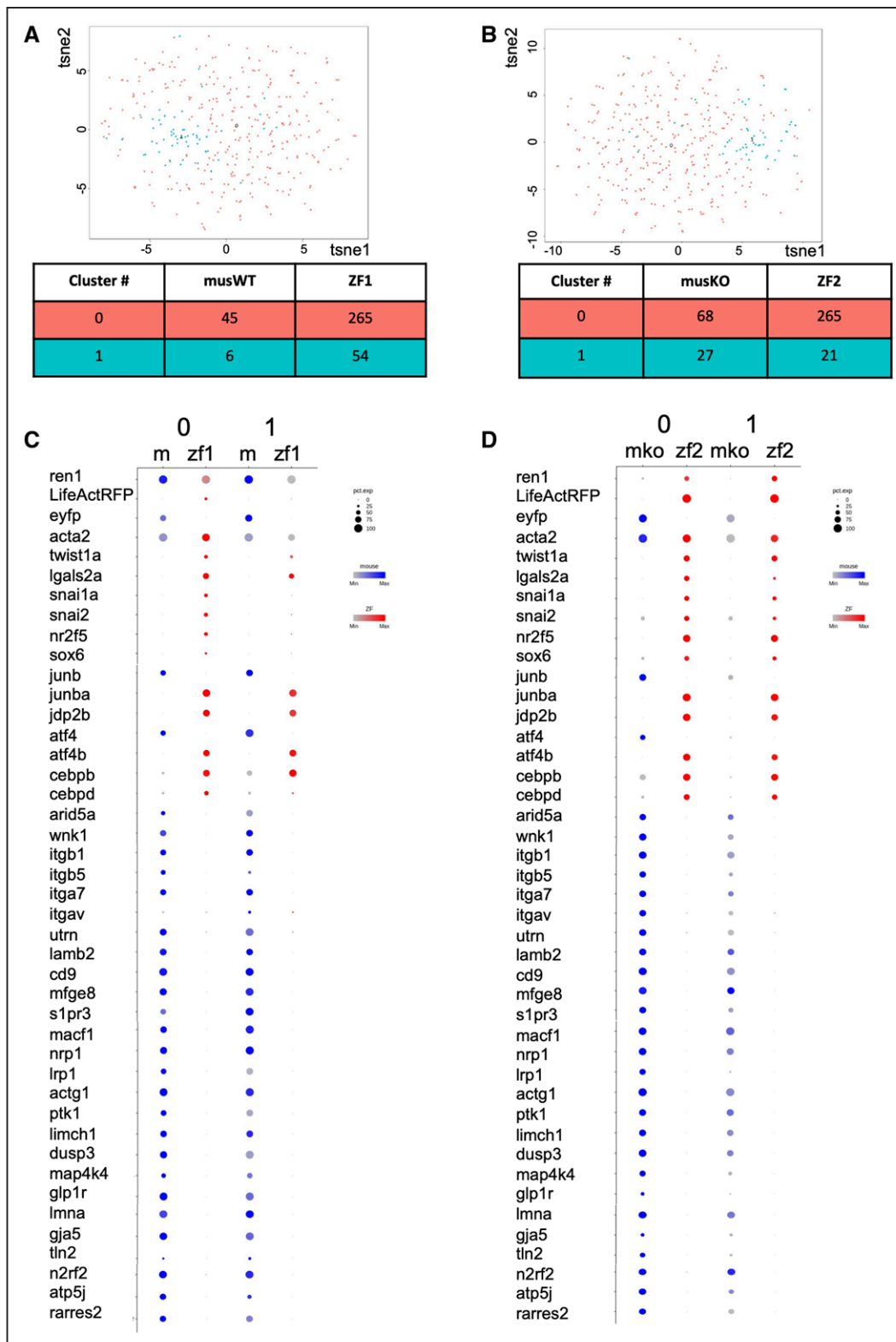


Figure 3. Merged expression matrices following canonical correlation analysis.

(A) Wild-type mouse and zebrafish juxtaglomerular cells (resolution 0.5) and (B) renin knockout mouse and zebrafish renin lineage cells (resolution 0.6). Associated tables give contributing cell numbers from respective matrices; (C and D) genes differentially expressed between respective mouse and zebrafish libraries, irrespective of genotype, are shown in dot plots.

recruited RLCs (Figure 3B). Dot plots show a number of transcripts, irrespective of genotype, which were mouse RLC-specific, including a number of integrins. The mouse

Ren1^{+/+} and *Ren1^{-/-}* libraries both showed significant enrichment of gene transcripts related to thyroid receptor binding (5.7-fold), regulation of focal adhesion assembly

(5.7-fold), and integrin binding (4.0-fold), as assessed by gene ontology analysis, compared with the respective zebrafish libraries. There was a 4.3-fold enrichment of gene transcripts associated with positive regulation of blood pressure in the mouse libraries, while both zebrafish libraries showed a 4-fold enrichment of gene transcripts associated with sprouting angiogenesis (Table 3).

DISCUSSION

Using the CRISPR/Cas9 system we targeted zebrafish *ren* exon 2 and generated multiple allelic variants. The survival of *ren*^{-/-} fish might reflect their aquatic environment, since homozygous *Ren1*^{c-/-} mice require daily administration of saline solution to prevent neonatal death.⁹ This suggests that transition to land created additional homeostatic challenges, possibly leading to the development of the macula densa in the metanephric kidney and baroreceptors.

Although *ren*^{-/-} larvae were completely viable, the delay in growth, late appearance of the swim bladder, and delayed glomerular fusion most likely resulted from an adverse effect on salt handling. Low salt in combination with Captopril resulted in complete loss of viability of *ren*^{-/-} larvae (compared with reduced survival of wild-type larvae in low salt and 0.1 mmol/L Captopril¹⁶). Renin is increased in ion-poor fresh water,¹³ implicating renin functionality in salt absorption, but zebrafish larvae rely predominantly on the 5 types of ionocytes in their gills and skin, which provide alternative routes for establishing salt homeostasis, until the kidneys are fully developed.⁴² The Na⁺Cl⁻ co-transporter-rich NCC ionocytes are thought to be responsive to Ang II,⁴³ though this does not explain the loss of viability of *ren*^{-/-} larvae (which presumably lack Ang II), in low salinity plus Captopril.

In larvae, renin expression is limited to the AMA region, which supplies the swim bladder. We saw no increase

in renin reporter expression in the AMA of *ren*^{-/-} larvae grown in CW. However, optogenetic ablation of the RLCs, caused an increase in arterial diameter, suggesting loss of tone. The observed increase in lumen diameter would correspond to ≈22% increase in lumen cross-sectional area. To our knowledge, this is the first direct demonstration of contractile functionality in RLCs, in vivo, though it does not suggest that renin or Ang II are involved per se, rather that the cells have dual functionality. This should be explored in the mesonephric and metanephric kidney.

To interrogate renin functionality in our adult mutants, our collaborators (Attoquant Diagnostic GmbH, Vienna, Austria) developed an indirect renin assay and demonstrated a complete absence of Ang I and Ang II in the mesonephric kidneys of adult *ren*^{-/-} zebrafish. Normal levels of the metabolites were found in mesonephric kidneys from *ren*^{Δ9/Δ9} and *ren*^{K1/K1} confirming that neither removal nor alteration of this glycosylation site dramatically affects protein folding or activity of renin. The glycosylation sites are located towards the surface of the renin protein, which may explain the apparent flexibility in protein conformation.

Loss of a functional *ren* gene resulted in alterations to mesonephric kidney morphology—specifically cytoplasmic vacuolation of proximal tubular epithelium, but not renal degeneration.⁴⁴ Vacuolation of proximal tubule cells often indicates an osmotic imbalance due to increased solute transport across the cells.⁴⁵ However, an almost complete absence of detectable Ang II may have adverse effects on the proximal tubule where it normally stimulates sodium and water reabsorption.⁴⁶ Since vacuolation of proximal cells was also observed in the *Ren1*^{c-/-} mouse, this suggests a conserved response to the lack of renin, reflecting a common action of Ang II on proximal tubule ion/water transport across species and deserving further investigation. This contrasts with the absence of such a mechanism in the glomerular teleost.⁴⁷

Table 3. Gene Ontology Analyses Giving Fold Enrichment of Differentially Expressed Gene Transcripts Between Wild-Type or Renin Knockout Mouse and Zebrafish Libraries

GO term	Mus <i>Ren1</i> ^{+/+}	ZF <i>ren</i> ^{+/+}	Mus <i>Ren1</i> ^{-/-}	ZF <i>ren</i> ^{-/-}	Associated genes
Thyroid receptor binding	6.38	...	5.07	...	<i>Trip12</i> , <i>Arid5a</i> *, <i>Thrap3</i> , <i>Tacc1</i> *, <i>Brd8</i>
Integrin binding	3.78	...	4.29	...	<i>Utn</i> *, <i>Cd81</i> , <i>Cd9</i> *, <i>Emp2</i> , <i>Dmd</i> , <i>Lamb2</i> *, <i>Mfge8</i> *, <i>Nisch</i> *, <i>Gsk3b</i> , <i>S1pr3</i> *
Integrin complex	3.74	...	4.6	...	<i>Itgb1</i> *, <i>Itgb5</i> *, <i>Itgav</i> *, <i>1tga7</i> *
Regulation of focal adhesion assembly	5.59	...	5.8	...	<i>Rac1</i> , <i>Nrp1</i> *, <i>Vegfa</i> , <i>Iqgap1</i> , <i>Limch1</i> *, <i>Clasp2</i> , <i>Pten</i> , <i>Lrp1</i> *, <i>Actg1</i> *, <i>Ptk2</i> *, <i>Dusp3</i> *, <i>Macf1</i> *, <i>S100a10</i> , <i>Map4k4</i> *
Positive regulation of blood pressure	4.3	...	4.33	...	<i>Glp1r</i> *, <i>Wnk1</i> *, <i>Agtr1a</i> , <i>id2</i> , <i>Nr2f2</i> *, <i>Atp5j</i> *, <i>Rarres2</i> *
Actin cap	22.3	...	15.23	...	<i>Cald1</i> *, <i>Gsn</i> , <i>Actr2</i> *
Actin filament depolymerization	9.93	...	8.45	...	<i>Wdr1</i> *, <i>Gsn</i> , <i>Mical3</i> *, <i>Dstin</i> *
Actin filament polymerization	...	5.5	...	5.8	<i>capza1b</i> , <i>pfn2</i> , <i>pfn1</i> , <i>pfn2l</i> *, <i>tmsb4x</i> *, <i>lmod1b</i>
relaxation of smooth muscle	16.55	...	9.02	...	<i>Rgs2</i> , <i>Prkg1</i> *, <i>Slc8a1</i> *, <i>Gucy1a1</i> , <i>Mvri1</i>
Sprouting angiogenesis	...	4.16	...	4.82	<i>pgfb</i> , <i>pkma</i> , <i>cxc12b</i> , <i>vegfaa</i> , <i>rtn4a</i> , <i>atf4b</i> , <i>crema</i> , <i>lgals2a</i> *, <i>twist1a</i> *

GO indicates gene ontology; and ZF, zebrafish.
*Only transcribed in mouse or zebrafish, respectively.

During early mammalian kidney development, renin cells are expressed throughout the renal vasculature—only after birth are renin-expressing cells spatially restricted to the juxtaglomerular apparatus.⁴⁸ However, RLCs retain the ability to switch to an endocrine renin phenotype in response to physiological challenge.^{18,33,49,50} We questioned whether the lack of functional renin might simulate such a challenge and crossed the double-transgenic reporter line *Tg(ren:LifeAct-RFP, acta2:EGFP)* with *ren^{+/+}* and *ren^{-/-}* fish to assess the extent of RLCs in the mesonephric kidney. There was a dramatic recruitment of RLCs along the renal vasculature with concomitant decrease of EGFP expression in the mesonephric kidney of the *ren^{-/-}* zebrafish, as seen in the mouse.⁴⁸ RLCs may be recruited along the arterioles in an attempt to control ion concentration and/or blood volume. Obligate heterozygous fish carrying deletion or substitution of the exon 2 glycosylation site, in combination with the knockout allele complemented for loss of renin, as shown by the restoration of the banding pattern of afferent arterioles. This, together with the biochemical data, confirms that renin glycosylation in exon 2, though highly conserved, is not essential for renin activity.

Fluorescence-activated cell sorting of vascular and renin fluorescent reporter-expressing cells on *ren^{+/+}* or *ren^{-/-}* backgrounds proved to be a very effective method for isolating JG cells from the former and RLCs from the latter, where over 3-fold more cells expressed the RFP reporter. Cluster analysis of the merged zebrafish libraries clearly distinguished RLCs from smooth muscle cells, identifying numerous upregulated renin cell-specific transcription factors, including *cnot4b*, *twist1a*, *nr2f5*, *nkx3.2*, and *sox6*, or downregulated transcription factors (*cited4a*), regulators of signaling pathways including *angptl3* and *rgs5b*, and also *hmox1a*, *tnmd*, and *tfpia*. Several of these have been recognized previously as RLC-specific in the mouse.¹⁸

Sub-cluster analysis allowed us to identify differentially expressed genes distinguishing JG cells from RLCs. Increased expression of *cited4a*, *id1*, *dio1*, *nrarpa*, *nkx3.2*, and *tnfaip8l3* was seen in JG cells relative to RLCs, while RLCs exhibited increased *twist1a*, *cnot4b*, *cremb* and *fosl2* transcription-related factors and a large group of signaling factors including *igfbp5b*, *cnp1*, *alkal1*, *rgl1*, *angptl3*, *gpr137ba*, *vegfaa*, *pgfb*, and *gng2*. Pseudotime mapping indicated that cluster 0 may represent a transition stage between JG cells and RLCs. This suggests a possible de-differentiation and re-differentiation of RLC-derived smooth muscle cells as they become recruited. The overall response to renin knockout was confirmed by canonical correlation analysis of the merged libraries.

Comparison with mouse expression matrices allowed us to look for conserved and divergent expression profiles from respective *Ren^{+/+}* and *Ren^{-/-}* cells of the zebrafish and mouse. Irrespective of genotype, JG cells and RLCs from the zebrafish mesonephric kidney libraries expressed *snai1a*, *snai2*, *twist1a*, and *sox6*, all of which enable DNA-binding of transcription factors, but

none of these were transcribed to a significant extent in the mouse libraries. Equally irrespective of genotype, JG cells and RLCs from the mouse metanephric kidney libraries expressed transcripts associated with integrins and regulation of focal adhesion. This is highly suggestive that such functions have evolved in RLCs of higher mammals, along with their exposure to increasing blood pressure.⁵¹ Transcripts from the recently identified nuclear mechano-transducer, lamin A (*Lmna*), associated with the mouse JG cell baroreceptor,⁵² were also noticeably absent from zebrafish-derived RLCs, suggesting an additional control in land-based mammals.

In conclusion, despite the control of ion balance afforded to the zebrafish through ionocytes of the gills and skin, these studies reveal conservation of functions such as RLC recruitment and RAS involvement in proximal tubule function between the zebrafish and the mouse, while other functions, related to increased blood pressure, have evolved. The zebrafish is proving a valuable and tractable, vertebrate model for exploring mechanisms in the RAS and renin cell biology.

PERSPECTIVE

Ablation of renin lineage cells in the AMA of zebrafish larvae reveals dual functionality of the cells—both renin expression and contractility. This should be explored in the mesonephric and metanephric kidney. Targeted knockout of renin function is not lethal in zebrafish larvae, because sodium homeostasis is achieved by ionocytes in the gills. Following renin knockout, adult zebrafish show vacuolation of the proximal tubule and renin lineage cell recruitment in the mesonephric vasculature, both of which are seen in the metanephric kidney of the mouse, suggesting an ongoing requirement for renin in both species. Transcriptome analysis of renin lineage cells from zebrafish and mice reveal significant differences however—with mouse RLCs expressing transcripts associated with integrins and focal adhesion regulation. This suggests that such functions have evolved with transition to land, which created additional homeostatic challenges including increased blood pressure.

ARTICLE INFORMATION

Received October 19, 2021; accepted December 23, 2021.

Affiliations

Centre for Cardiovascular Science (S.H., L.M., S.R., C.B., C.B.B., A.A., Z.L., J.M.) and Centre for Inflammation Research (M.S.B., N.H.), The Queen's Medical Research Institute, The University of Edinburgh, United Kingdom. Now with DSM Nutritional Products Ltd, Switzerland (S.R.). Now with Strathclyde Institute of Pharmacy and Biomedical Sciences, University of Strathclyde, Glasgow, United Kingdom (C.B.B.). MRC Human Genetics Unit, Institute of Genetics and Molecular Medicine, University of Edinburgh, United Kingdom (N.H.). Veterinary Pathology, Royal (Dick) School of Veterinary Studies and The Roslin Institute, The University of Edinburgh, Easter Bush Campus, United Kingdom (J.d.P.). Department of Pediatrics, School of Medicine, University of Virginia, Charlottesville (A.D.G.M., M.L.S.S.-L., R.A.G.).

Acknowledgments

We wish to thank Dr John Wilson-Kanamori for assistance with bioinformatics analysis, and Dr Alessandro Brombin for assistance with construction of the zebrafish reference genome. We thank the QMRI aquarium staff for technical help; Jason Early and the UK Zebrafish Screening Facility; Xiuyin Liang for technical help; Attoquant Diagnostic GmbH, Vienna, Austria for angiotensin metabolite assays.

Sources of Funding

C. Brown, C.B. Buckley, S. Rider, and A. Assmus were supported by the British Heart Foundation Centre of Research Excellence Award (RE/08/001/23904); S. Hoffmann by MRC/EPSRC DTA OPTIMA EP/L016559/1; L. Mullins by the BHF CoRE and Kidney Research UK (RP_026_20180305). R.A. Gomez and M.L.S. Sequeira-Lopez are supported by National Institutes of Health Grants (DK 096373, DK 116718, DK 116196, and HL 148044).

Disclosures

None.

REFERENCES

- Minuth M, Hackenthal E, Poulsen K, Rix E, Taugner R. Renin immunocytochemistry of the differentiating juxtaglomerular apparatus. *Anat Embryol (Berl)*. 1981;162:173–181. doi: 10.1007/BF00306489
- Celio MR, Groscurth P, Inagami T. Ontogeny of renin immunoreactive cells in the human kidney. *Anat Embryol (Berl)*. 1985;173:149–155. doi: 10.1007/BF00316297
- Richoux JP, Amsaguine S, Grignon G, Bouhnik J, Menard J, Corvol P. Earliest renin containing cell differentiation during ontogenesis in the rat. An immunocytochemical study. *Histochemistry*. 1987;88:41–46. doi: 10.1007/BF00490165
- Gomez RA, Norwood VF. Developmental consequences of the renin-angiotensin system. *Am J Kidney Dis*. 1995;26:409–431. doi: 10.1016/0272-6386(95)90487-5
- Reddi V, Zaglul A, Pentz ES, Gomez RA. Renin-expressing cells are associated with branching of the developing kidney vasculature. *J Am Soc Nephrol*. 1998;9:63–71. doi: 10.1681/ASN.V9163
- Guron G, Friberg P. An intact renin-angiotensin system is a prerequisite for normal renal development. *J Hypertens*. 2000;18:123–137. doi: 10.1097/00004872-200018020-00001
- Tufro-McReddie A, Romano LM, Harris JM, Ferder L, Gomez RA. Angiotensin II regulates nephrogenesis and renal vascular development. *Am J Physiol*. 1995;269(1 pt 2):F110–F115. doi: 10.1152/ajprenal.1995.269.1.F110
- Pentz ES, Moyano MA, Thornhill BA, Sequeira Lopez ML, Gomez RA. Ablation of renin-expressing juxtaglomerular cells results in a distinct kidney phenotype. *Am J Physiol Regul Integr Comp Physiol*. 2004;286:R474–R483. doi: 10.1152/ajpregu.00426.2003
- Takahashi N, Lopez ML, Cowhig JE Jr, Taylor MA, Hatada T, Riggs E, Lee G, Gomez RA, Kim HS, Smithies O. Ren1c homozygous null mice are hypotensive and polyuric, but heterozygotes are indistinguishable from wild-type. *J Am Soc Nephrol*. 2005;16:125–132. doi: 10.1681/ASN.2004060490
- Yanai K, Saito T, Kakinuma Y, Kon Y, Hirota K, Taniguchi-Yanai K, Nishijo N, Shigematsu Y, Horiguchi H, Kasuya Y, et al. Renin-dependent cardiovascular functions and renin-independent blood-brain barrier functions revealed by renin-deficient mice. *J Biol Chem*. 2000;275:5–8. doi: 10.1074/jbc.275.1.5
- Fournier D, Luft FC, Bader M, Ganten D, Andrade-Navarro MA. Emergence and evolution of the renin-angiotensin-aldosterone system. *J Mol Med (Berl)*. 2012;90:495–508. doi: 10.1007/s00109-012-0894-z
- Armesto P, Cousin X, Salas-Leiton E, Asensio E, Machado M, Infante C. Molecular characterization and transcriptional regulation of the renin-angiotensin system genes in Senegalese sole (*Solea senegalensis* Kaup, 1858): differential gene regulation by salinity. *Comp Biochem Physiol A Mol Integr Physiol*. 2015;184:6–19. doi: 10.1016/j.cbpa.2015.01.021
- Hoshijima K, Hirose S. Expression of endocrine genes in zebrafish larvae in response to environmental salinity. *J Endocrinol*. 2007;193:481–491. doi: 10.1677/JOE-07-0003
- Kumai Y, Perry SF. Mechanisms and regulation of Na(+) uptake by freshwater fish. *Respir Physiol Neurobiol*. 2012;184:249–256. doi: 10.1016/j.resp.2012.06.009
- Kumai Y, Bernier NJ, Perry SF. Angiotensin-II promotes Na+ uptake in larval zebrafish, *Danio rerio*, in acidic and ion-poor water. *J Endocrinol*. 2014;220:195–205. doi: 10.1530/JOE-13-0374
- Rider SA, Mullins LJ, Verdon RF, MacRae CA, Mullins JJ. Renin expression in developing zebrafish is associated with angiogenesis and requires the Notch pathway and endothelium. *Am J Physiol Renal Physiol*. 2015;309:F531–F539. doi: 10.1152/ajprenal.00247.2015
- Rider SA, Christian HC, Mullins LJ, Howarth AR, MacRae CA, Mullins JJ. Zebrafish mesonephric renin cells are functionally conserved and comprise two distinct morphological populations. *Am J Physiol Renal Physiol*. 2017;312:F778–F790. doi: 10.1152/ajprenal.00608.2016
- Brunskill EW, Sequeira-Lopez ML, Pentz ES, Lin E, Yu J, Aronow BJ, Potter SS, Gomez RA. Genes that confer the identity of the renin cell. *J Am Soc Nephrol*. 2011;22:2213–2225. doi: 10.1681/ASN.2011040401
- Lin EE, Sequeira-Lopez ML, Gomez RA. RBP-J in FOXD1+ renal stromal progenitors is crucial for the proper development and assembly of the kidney vasculature and glomerular mesangial cells. *Am J Physiol Renal Physiol*. 2014;306:F249–F258. doi: 10.1152/ajprenal.00313.2013
- Liang P, Jones CA, Bisgrove BW, Song L, Glenn ST, Yost HJ, Gross KW. Genomic characterization and expression analysis of the first nonmammalian renin genes from zebrafish and pufferfish. *Physiol Genomics*. 2004;16:314–322. doi: 10.1152/physiolgenomics.00012.2003
- Parichy DM, Elizondo MR, Mills MG, Gordon TN, Engeszer RE. Normal table of postembryonic zebrafish development: staging by externally visible anatomy of the living fish. *Dev Dyn*. 2009;238:2975–3015. doi: 10.1002/dvdy.22113
- Diep CQ, Peng Z, Ukah TK, Kelly PM, Daigle RV, Davidson AJ. Development of the zebrafish mesonephros. *Genesis*. 2015;53:257–269. doi: 10.1002/dvg.22846
- Zhou W, Boucher RC, Bollig F, Englert C, Hildebrandt F. Characterization of mesonephric development and regeneration using transgenic zebrafish. *Am J Physiol Renal Physiol*. 2010;299:F1040–F1047. doi: 10.1152/ajprenal.00394.2010
- Diep CQ, Ma D, Deo RC, Holm TM, Naylor RW, Arora N, Wingert RA, Bollig F, Djordjevic G, Lichman B, et al. Identification of adult nephron progenitors capable of kidney regeneration in zebrafish. *Nature*. 2011;470:95–100. doi: 10.1038/nature09669
- Westerfield M. *A guide for the laboratory use of zebrafish danio (brachydanio rerio)*. University of Oregon Press; 2007.
- Brinkman EK, Chen T, Amendola M, van Steensel B. Easy quantitative assessment of genome editing by sequence trace decomposition. *Nucleic Acids Res*. 2014;42:e168. doi: 10.1093/nar/gku936
- Perner B, Englert C, Bollig F. The Wilms tumor genes wt1a and wt1b control different steps during formation of the zebrafish pronephros. *Dev Biol*. 2007;309:87–96. doi: 10.1016/j.ydbio.2007.06.022
- Whitesell TR, Kennedy RM, Carter AD, Rollins EL, Georgijevic S, Santoro MM, Childs SJ. An α -smooth muscle actin (acta2/asm) zebrafish transgenic line marking vascular mural cells and visceral smooth muscle cells. *PLoS One*. 2014;9:e90590. doi: 10.1371/journal.pone.0090590
- Buckley C, Carvalho MT, Young LK, Rider SA, McFadden C, Berlage C, Verdon RF, Taylor JM, Girkin JM, Mullins JJ. Precise spatio-temporal control of rapid optogenetic cell ablation with mem-KillerRed in Zebrafish. *Sci Rep*. 2017;7:5096. doi: 10.1038/s41598-017-05028-2
- Lawton PF, Lee MD, Saunter CD, Girkin JM, McCarron JG, Wilson C. VasoTracker, a low-cost and open source pressure myograph system for vascular physiology. *Front Physiol*. 2019;10:99. doi: 10.3389/fphys.2019.00099
- McCampbell KK, Springer KN, Wingert RA. Atlas of cellular dynamics during zebrafish adult kidney regeneration. *Stem Cells Int*. 2015;2015:547636. doi: 10.1155/2015/547636
- Schindelin J, Arganda-Carreras I, Frise E, Kaynig V, Longair M, Pietzsch T, Preibisch S, Rueden C, Saalfeld S, Schmid B, et al. Fiji: an open-source platform for biological-image analysis. *Nat Methods*. 2012;9:676–682. doi: 10.1038/nmeth.2019
- Gomez RA, Belyea B, Medrano S, Pentz ES, Sequeira-Lopez ML. Fate and plasticity of renin precursors in development and disease. *Pediatr Nephrol*. 2014;29:721–726. doi: 10.1007/s00467-013-2688-0
- Butler A, Hoffman P, Smibert P, Papalexi E, Satija R. Integrating single-cell transcriptomic data across different conditions, technologies, and species. *Nat Biotechnol*. 2018;36:411–420. doi: 10.1038/nbt.4096
- Trapnell C, Cacchiarelli D, Grimsby J, Pokharel P, Li S, Morse M, Lennon NJ, Livak KJ, Mikkelsen TS, Rinn JL. The dynamics and regulators of cell fate decisions are revealed by pseudotemporal ordering of single cells. *Nat Biotechnol*. 2014;32:381–386. doi: 10.1038/nbt.2859
- Bolger AM, Lohse M, Usadel B. Trimmomatic: a flexible trimmer for Illumina sequence data. *Bioinformatics*. 2014;30:2114–2120. doi: 10.1093/bioinformatics/btu170

37. Patro R, Duggal G, Love MI, Irizarry RA, Kingsford C. Salmon provides fast and bias-aware quantification of transcript expression. *Nat Methods*. 2017;14:417–419. doi: 10.1038/nmeth.4197
38. Sonesson C, Love MI, Robinson MD. Differential analyses for RNA-seq: transcript-level estimates improve gene-level inferences. *F1000Res*. 2015;4:1521. doi: 10.12688/f1000research.7563.2
39. DeLaughter DM. The use of the Fluidigm C1 for RNA expression analyses of single cells. *Curr Protoc Mol Biol*. 2018;122:e55. doi: 10.1002/cpmb.55
40. Pentz ES, Lopez ML, Cordaillat M, Gomez RA. Identity of the renin cell is mediated by cAMP and chromatin remodeling: an in vitro model for studying cell recruitment and plasticity. *Am J Physiol Heart Circ Physiol*. 2008;294:H699–H707. doi: 10.1152/ajpheart.01152.2007
41. Watanabe H, Martini AG, Brown EA, Liang X, Medrano S, Goto S, Narita I, Arend LJ, Sequeira-Lopez MLS, Gomez RA. Inhibition of the renin-angiotensin system causes concentric hypertrophy of renal arterioles in mice and humans. *JCI Insight*. 2021;6:e154337. doi: 10.1172/jci.insight.154337
42. Pittman K, Yufera M, Pavlidis M, Geffen A, Koven W, Ribeiro L, Zambonino-Infante J, Tandler A. Fantastically plastic: fish larvae equipped for a new world. *Rev Aquac*. 2013;5:S224–S267. doi: 10.1111/raq.12034
43. Guh YJ, Hwang PP. Insights into molecular and cellular mechanisms of hormonal actions on fish ion regulation derived from the zebrafish model. *Gen Comp Endocrinol*. 2017;251:12–20. doi: 10.1016/j.ygcen.2016.08.009
44. Bendele A, Seely J, Richey C, Sennello G, Shopp G. Short communication: renal tubular vacuolation in animals treated with polyethylene-glycol-conjugated proteins. *Toxicol Sci*. 1998;42:152–157. doi: 10.1006/toxs.1997.2396
45. Dickenmann M, Oettl T, Mihatsch MJ. Osmotic nephrosis: acute kidney injury with accumulation of proximal tubular lysosomes due to administration of exogenous solutes. *Am J Kidney Dis*. 2008;51:491–503. doi: 10.1053/ajkd.2007.10.044
46. Horita S, Nakamura M, Shirai A, Yamazaki O, Satoh N, Suzuki M, Seki G. Regulatory roles of nitric oxide and angiotensin II on renal tubular transport. *World J Nephrol*. 2014;3:295–301. doi: 10.5527/wjn.v3.i4.295
47. Zucker A, Nishimura H. Renal responses to vasoactive hormones in the aglomerular toadfish, *Opsanus tau*. *Gen Comp Endocrinol*. 1981;43:1–9. doi: 10.1016/0016-6480(81)90024-1
48. Sauter A, Machura K, Neubauer B, Kurtz A, Wagner C. Development of renin expression in the mouse kidney. *Kidney Int*. 2008;73:43–51. doi: 10.1038/sj.ki.5002571
49. Lopez ML, Gomez RA. The renin phenotype: roles and regulation in the kidney. *Curr Opin Nephrol Hypertens*. 2010;19:366–371. doi: 10.1097/MNH.0b013e32833aff32
50. Sequeira López ML, Pentz ES, Nomasa T, Smithies O, Gomez RA. Renin cells are precursors for multiple cell types that switch to the renin phenotype when homeostasis is threatened. *Dev Cell*. 2004;6:719–728. doi: 10.1016/s1534-5807(04)00134-0
51. Mohamed TH, Watanabe H, Kaur R, Belyea BC, Walker PD, Gomez RA, Sequeira-Lopez MLS. Renin-expressing cells require β 1-Integrin for survival and for development and maintenance of the renal vasculature. *Hypertension*. 2020;76:458–467. doi: 10.1161/HYPERTENSIONAHA.120.14959
52. Watanabe H, Belyea BC, Paxton RL, Li M, Dzamba BJ, DeSimone DW, Gomez RA, Sequeira-Lopez MLS. Renin cell baroreceptor, a nuclear mechanotransducer central for homeostasis. *Circ Res*. 2021;129:262–276. doi: 10.1161/CIRCRESAHA.120.318711